Contents lists available at http://qu.edu.iq

Al-Qadisiyah Journal for Engineering Sciences

Journal homepage: http://qu.edu.iq/journaleng/index.php/JQES

Corrosion inhibition performance of 2- fluorophenyl-2, 5 dithiohydrazodicarbonamide for copper in 3.5%NaCl Media: Experimental and Monte Carlo insights

Mothana Ghazi Kadhim AlFalah [a, *], ***Murat Saracoglu*** [b], ***Mehmet Izzettin Yilmazer*** [c], ***and Fatma Kandemirli*** [d]

[a] *Kastamonu University, Faculty of Engineering and Architecture, Metallurgy and Materials Engineering Department, 37150, Kastamonu, Türkiye*
[b] *Erciyes University, Faculty of Education, 38039, Kayseri, Türkiye*
[c] *Erciyes University, Faculty of Science, Department of Chemistry, 38039, Kayseri, Türkiye*
[d] *Kastamonu University, Faculty of Engineering and Architecture, Biomedical Engineering Department, 37150, Kastamonu, Türkiye*

ARTICLE INFO

Article history:
Received 3 March 2023
Received in revised form 15 April 2023
Accepted 25 July 2023

Keywords:
Copper
Corrosion resistance
EIS
Langmuir
Monte Carlo simulation

ABSTRACT

Most industries struggle with corrosion. Corrosion inhibitors are needed in these sectors. Eco-friendly corrosion inhibitors should be effective even at low concentrations. In this work, the compound 2-Fluorophenyl-2, 5- dithiohydrazodicarbonamide (2F-TSC) was utilized as a corrosion inhibitor for copper in a 3.5% NaCl solution. The inhibitor efficiency was calculated by using a series of electrochemical methods like, open circuit potential (OCP), potentiodynamic polarization (PDP), and electrochemical impedance spectroscopy (EIS). All tests have been done in a stagnant condition. The results show that the compound 2F-TSC looked to be of mixed type. Furthermore, the maximum inhibitor efficiency was reached at 99.2% at 10^{-2} M 2F-TSC and 5 h. The adsorption of 2F-TSC on the copper surface in 3.5% NaCl obeyed the Langmuir isotherm with a negative value of the standard Gibbs free energy of adsorption of -35.4 kJ/mol (chemisorption and physisorption). SEM, EDX, and AFM confirmed the presence of 2F-TSC on the surface of copper. The adsorption of the inhibitor molecules on the Cu (111) surface was further verified by a Monte Carlo simulation study. The results approved that the 2F-TSC can be utilized as a corrosion inhibitor for copper in an aggressive solution (3.5% NaCl).

1. Introduction

Certainly, copper is a commonly used metal in various industries due to its high electrical conductivity, ductility, and malleability. Copper metals are often used in pipelines, and heat transfer tubes are also something to think about [1]. However, its susceptibility to corrosion can be a cause for concern. When exposed to sodium chloride, which is a common component in many environments such as saltwater and road salt, copper can undergo a process called corrosion. This is because the chloride ions react with the copper atoms, causing them to lose electrons and form copper ions. These copper ions then combine with water molecules to form copper (II) hydroxide, which appears as a greenish-blue crust or powder on the surface

* *Corresponding author.*
E-mail address: *muthanakadhem@yahoo.com* (Mothana G. K. AlFalah)

https://doi.org/10.30772/qjes.2023.178995

of the copper. Over time, the corrosion process can weaken the metal and cause structural damage. It is important to take preventative measures, such as using coatings, corrosion inhibitors, and alloys, to minimize the risk of copper corrosion in sodium chloride environments [2–5]. In recent years, it has been found that inhibitors are the best way to protect metals from alkaline corrosion. They work better than cathodic and anodic protection, alloying, covering, and other common methods [6]. Organic inhibitors are often used to block light from getting through to metal surfaces. Most effective are organic molecules with highly electronic heteroatoms (like P, S, N, and O) or heteroatoms with an aromatic ring [7,8]. Also, molecules with pi electrons and functional groups like -N=N-, -C=N-, and >NH often have qualities that prevent corroding [9,10]. In alkaline settings where copper is likely to rust, the best corrosion fighters are N- and S- heterocyclic molecules. Because they have been around for a long time, organic molecules are by far the most advanced and cost-effective tools for making things. The rest, on the other hand, are poisonous and bad for the environment. There have been attempts all over the world to find a rust inhibitor that is effective, cheap, and safe [11–13]. Dithiohydrazodicarbonamides have shown that they can be used in many ways as medications [14]. Because they work well as copper corrosion inhibitors in NaCl solutions, these ligands are also well known for their anti-corrosion properties [15].

The corrosion of copper and mild steel in aqueous chloride systems (HCl or NaCl) has been shown to be inhibited by a wide variety of organic compounds [16,17]. Corrosion inhibitors made of amines, their dithiocarbamates, and Cu or Fe complexes have been used successfully in these systems [2,18,19]. The effectiveness of the inhibitor was further enhanced when thiosemicarbazide was combined with phenyl isothiocyanate to create 1-phenyl,2,5- dithiohydrazodicarbonamide. In our previous work, we synthesized and examined 2-Flouro pheyl-2,5-dithiohydraodicarbonamide (2F-TSC) as a corrosion inhibitor for mild steel in 1 M HCl solution with excellent results [14]. Therefore it has been encouraged to investigate this compound (2F-TSC) with different metals and solutions, such as copper in a 3.5% NaCl solution. In the present work, 2F-TSC has been tested as a corrosion inhibitor for copper in 3.5% NaCl solution. The inhibitor efficiency was calculated by electrochemical methods such as linear polarization resistance (LPR), potentiodynamic polarization (PDP), and electrochemical impedance spectroscopy (EIS). The surface profile of the copper was tested with a scanning electron microscope (SEM), an energy dispersive X-ray spectroscopy (EDX), and an atomic force microscope (AFM) with and without the corrosion inhibitor (2F-TSC). Monte Carlo models have been done to show how tried anti-corrosion agents bind to surfaces. Structure

2. Materials and Methods

2.1 Materials and preparation of the samples

A copper bar has been provided from a local market with a chemical composition of 99.9% Cu (%Wt). Cylindrical specimens having a diameter of 1 cm and a length of 3 cm were prepared from copper bars. The samples were placed in epoxy resin with a total exposed surface area of 785 cm^2 after being linked from the back using copper wire. Silicon carbide sheets ranging in grit from 600 up to 2500 grit were used to achieve the mirror sheen on the sample surfaces. Polished samples were then washed twice in acetone and double-distilled water and kept until dried by air at room temperature. 2-Flouro pheyl-2,5-dithiohydraodicarbonamide (2F-TSC) has been synthesized and characterized in detail in our previous work (see Fig.1) [14]. The copper has been utilized to investigate the corrosion resistance of 3.5% sodium chloride as a free-corrosion inhibitor and in the existence of the corrosion inhibitor 2F-TSC.

The research solution for copper in 3.5% NaCl was made using 35 g of NaCl dissolved in distilled water and 2F-TSC. The most powerful inhibitor solution (10^{-2} M) was made by soaking the amount of 2F-TSC that was needed in 3.5% NaCl. The dilution method was used to make the inhibitor media with lower amounts (10^{-5}, 10^{-4}, and 10^{-3} M).

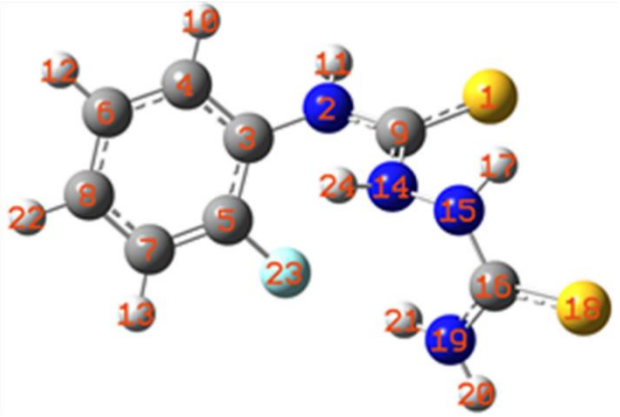

Figure 1. 2-Flouro pheyl-2,5-dithiohydraodicarbonamide (2F-TSC) structure [14]

2.2 corrosion tests

The three-electrode cell utilized for all experiments consisted of a working electrode (copper), a reference electrode made of silver/silver chloride (3 M NaCl), and a counter electrode made of platinum. A potentiostat (IVIUM Technologies, Instrument: B08024, Software: 2699) was used for all testing. Before beginning the EIS, LPR, and PDP, the Cu was immersed in the test solution (3.5% sodium chloride as a free-corrosion inhibitor and the existence of 2F-TSC) for one hour in order to create a generally consistent state and construct an OCP. In EIS tests, AC signals with an intensity of 0.005 V and a frequency between 100,000 Hz and 0.02 Hz were used. Using the comparable circuit, the information that was gathered was judged. The LPR readings were taken at a rate of 1 mV/s from the cathodic potential to the anodic potential ±0.01 V_{OCP}. For PDP tests, a voltage of ±0.250 V_{OCP} at a scan rate of 1 mV/s was used. All tests were run three times to guarantee accuracy and reproducibility.

2.3 Surface studies

The goal of this study was to learn more about how the surface of alkaline samples changes before and after an inhibitor is added. The Cu specimens were originally immersed in 3.5% NaCl in a blank at 298 K, where the concentration of 2F-TSC was 10^{-2} M. The copper samples were removed from the test solution after 72 hours and allowed to dry. All the parameters and types of instruments for SEM, EDX, and AFM have been mentioned in detail in our previous work [14,20].

2.4 Monte Carlo simulation

The Monte Carlo (MCS) models were executed using the adsorption finder feature of Material Studio 2017 to investigate the chemical interactions

between the adsorbate and substrate. The aqueous component of the system consisted of 500 molecules of H_2O, 5 ions of Na^+, 5 ions of Cl^-, and a Cu (111) surface. The fabrication of the box cell involved the slicing of the copper surface (111) into seven copper layers. The selection of the Cu surface (111) preceded this action. The supercell was constructed within a spatial extent of 13 by 13 units. It is necessary to ensure that the size of the vacuum is sufficient to prevent any interference with the regularity of the atoms in the bottom layer of the surface, caused by the non-bonded calculation of the adsorbate. Consequently, a vacuum slab with a thickness of 50 and oriented along the C-axis was constructed using Crystal Builder. The Ewald summation technique was employed to compute the electrostatic potential energy, while the atom-based approach was utilized to determine the van der Waals potential energy. The COMPASS force field, which is optimized for atomistic simulation studies in condensed phases, was employed to alter the configuration of all pertinent components of the system. The dimensions of the box, which was created using periodic boundary conditions, are 29.78 × 29.78 × 62.16 $Å^3$. Forcite was employed to perform geometry optimization.

3. Results and discussion

3.1 OCP, PDP, and LPR

Both a blank solution and 2F-TSC were used to test the OCP of Cu for 60 minutes. Figure 2 shows the results obtained for compound 2F-TSC. The OCP value swinging negatively at the start of immersion in the inhibitor-free solution may be due to the development of an oxide layer on the surface of the copper. OCP measurements get more and more negative as the immersion time goes on, indicating that the Cu chloride is forming and the oxide coating is disintegrating [21–23]. The potential at the conclusion of the test shifts in a more positive direction when an inhibitor is present, with the exception of doses 10^{-2} M 2F-TSC. This result could be brought about by the inhibitor molecules producing a shielding layer after attaching to the copper active sites [15,24,25].

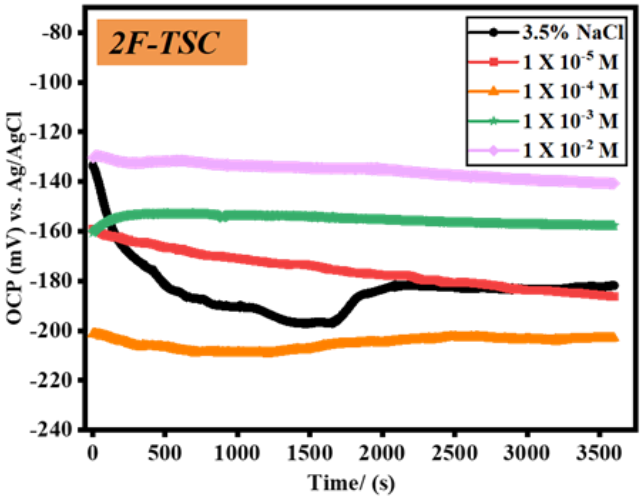

Figure 2. Open circuit potential without and within the presence of 2F-TSc in 3.5% NaCl

Figure 3 (A–B) shows PDP plots for copper that has not been blocked and copper that has been blocked by different concentrations of 2F-TSC in 3.5% NaCl at 1 and 5 hours.

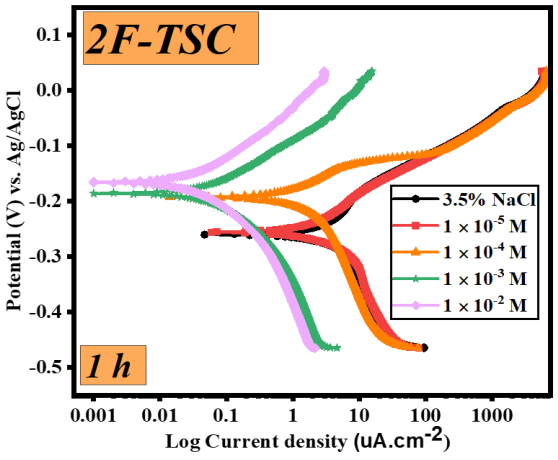

(A)

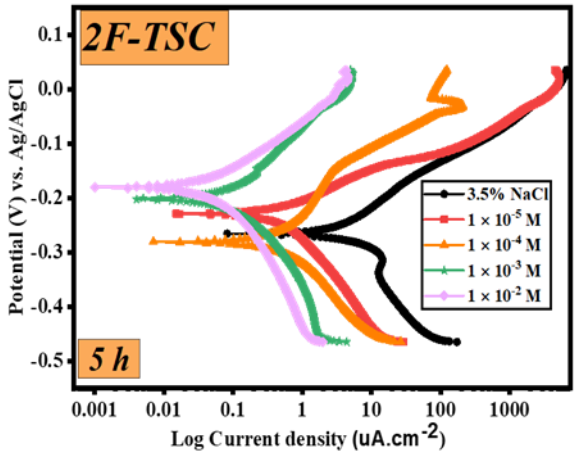

(B)

Figure 3. Potentialdynamic polarization for 2F-TSC as a blank and with different concentrations at immersion time 1 h (A) and 5 h (B).

It can be noted that as the concentration of the investigated inhibitor went up, both the anodic and cathodic curves changed significantly. This caused the current density to go down, which shows that the tested compounds have an inhibiting effect. Also, it was seen that the Tafel slope (βc) changed when 2F-TSC was added. This is because basic blocking slows down the activity of cathodic sites on a copper surface, which causes oxygen reduction to slow down as well (Table 1). With the addition of the inhibitor, the values of the anodic Tafel slopes (βa) varied somewhat, showing that these molecules were initially adsorbed to the basic copper surface and hampered by blocking the metal surface reaction sites. The inhibitor did not modify the corrosion mechanism, according to Tafel slope values. Tested chemicals inhibit active sites on the electrode surface by adsorbing inhibitor molecules [14,20].

Table 1. PDP and LPR for copper in 3.5% sodium chloride solution without and with the existence of 2F-TSC at immersion time 1 and 5 h.

	time	Cons. (M)	E_{corr} (V)	i_{corr} ($\mu A.cm^{-2}$)	$-\beta_c$ (V/dec)	β_a (V/dec)	θ	% IE	R_{lp} ($\Omega.cm^2$)	θ	% IE
2-F-TSC	*1 h*	BLANK	-0,2607	3,91	0,308	0,070	-----	-----	04460,04	-----	----
		1×10^{-5}	-0,2554	3,09	0,294	0,066	0,207	20,8	06065,16	0,264	26,5
		1×10^{-4}	-0,1928	1,56	0,289	0,073	0,601	60,2	0011775	0,621	62,1
		1×10^{-3}	-0,1857	0,09	0,221	0,082	0,976	97,7	0235343	0,981	98,1
		1×10^{-2}	-0,1657	0,06	0,235	0,099	0,984	98,5	0421702	0,989	98,9
	5 h	BLANK	-0,2658	7,88	0,190	0,071	-----	-----	02753,69	-----	----
		1×10^{-5}	-0,2297	0,86	0,168	0,057	0,8908	89,1	24766,75	0,889	88,9
		1×10^{-4}	-0,2812	0,37	0,155	0,074	0,9530	95,3	32883,23	0,916	91,6
		1×10^{-3}	-0,2021	0,18	0,227	0,122	0,9771	97,7	0179608	0,985	98,5
		1×10^{-2}	-0,1806	0,09	0,233	0,097	0,9885	98,8	336843,5	0,992	99,2

Table 2. EIS for copper in 3.5% NaCl solution with absence and with the present of 2F-TSC at immersion time 1 and 5 h.

	Time	Cont. (M)	R_S ($\Omega.cm^2$)	R_{p1} ($\Omega.cm^2$)	CPE ($\mu F.cm^{-2}$)	n	W $\Omega^{-1}.cm^{-2}$ $s^{0.5}$	R_{pT} ($\Omega.cm^2$)	% IE
2-F-TSC	*1 h*	BALNK	6,9	002020,5	2907	0,48	2,334	002020,5	------
		1×10^{-5}	8,1	002980,7	225	0,75	2,132	002980,7	32,2
		1×10^{-4}	7,7	006025,3	11,8	0,85	1,782	006025,3	66,5
		1×10^{-3}	9,6	173309,2	0,73	0,94	1,236	173309,2	98,8
		1×10^{-2}	8,9	321552,5	0,49	0,97	0,92	321552,5	99,4
	5 h	BLANK	5,9	0002255	17,1	0,88	1,892	0002255	-----
		1×10^{-5}	09	022495,9	06,4	0,89	1,143	022495,9	89,9
		1×10^{-4}	8,8	024409,9	05,2	0,90	0,991	024409,9	90,8
		1×10^{-3}	09	076735,3	04,1	0,95	0,612	076735,3	97,1
		1×10^{-2}	09	209697,1	00,6	0,97	0,406	209697,1	98,9

Additionally, compared to copper which was not inhibited, the current densities were much lower in the presence of the inhibitor. When copper was exposed to 10^{-2} M 2F-TSC during a 1-hour immersion period, the reduction went from 3.91 $\mu A.cm^{-2}$ for unprotected copper to 0.06 $\mu A.cm^{-2}$. This can be a result of inhibitor molecules adhering to the metallic surface, stopping or delaying the action of aggressive ions like Cl^- to assault the surface. [26]. Moreover, the corrosion potential ECorr values shifted towards more positive values when the inhibitor 2F-TSC concentration increased (Fig. 3 (A), Table 1). It is hypothesized that the potential value of corrosion is influenced by the rivalry between the suppression of cathodic and anodic processes [27]. Figure 3 (B) shows PDP plots for copper that has not been shielded and copper that has been stopped from reacting with different amounts of 2F-TSC in 3.5% NaCl for 5 hours. There have been some interesting outcomes. It can be seen that the current densities increased more for exposed copper as the duration of exposure grew. This is because the rate of copper dissociation and oxygen reduction also increased with exposure time. But the current levels have dropped sharply, even though there is less 2F-TSC around (Table1). In other words, the effectiveness of the inhibitor for 2F-TSC went from 20.8% at a concentration of 10^{-5} M and a time of exposure of 1 h to 89.1% after 5 h. However the most effective inhibitor was 98.8% when 2F-TSC was present at a concentration of 10^{-5} M for 5 hours.

It was hypothesized that the longer a copper surface remained submerged in an inhibitor solution, the more of its surface would be coated by molecules of the solution. Furthermore, the inclusion of inhibitors has altered the values of corrosion potential Ecorr more favorably towards the immunity zone. The presence of inhibitor 2F-TSC caused a shift from -0.2658 V to -0.1806 V in the copper's uninhibited state. Prior research has established that inhibitors may be classified as cathodic or anodic types if the corrosion potential values of said inhibitors exceed 0.085 V. Conversely, inhibitors may be categorized as mixed types if the aforementioned moves are less than 0.085 V [28]. The findings presented in Table 1 indicate that the displacements observed for corrosion potential values following a 5-hour submerged period do not exceed 0.085 V. Thus, it can be inferred that the 2F-TSC exhibited characteristics of a corrosion inhibitor with mixed inhibition properties.

The LPR results show In Table.1 that the polarization resistance was increased for uninhibited copper from 4460.4 $\Omega.cm^2$ to 421702 $\Omega.cm^2$ at immersion time 1 h with the existence of 2F-TSC at 1×10^{-2} M. Furthermore, it can be noticed that the resistance was increased at 5 h immersion time for unprotected copper from 2753.7 $\Omega.cm^2$ to 336843.5 $\Omega.cm^2$ with presence of 2F-TSC. This suggests that $1/R_{LPR}$ value is purely proportional to the i°_{corr} . It is noteworthy that the outcomes obtained from the implementation of OCP, PDP, and LPR methodologies are insufficient in terms of investigating the effectiveness of corrosion inhibitors.

Electrochemical impedance spectroscopy (EIS) was performed. The IE_{PDP} percentage and IE_{LPR} percentage values were determined through the

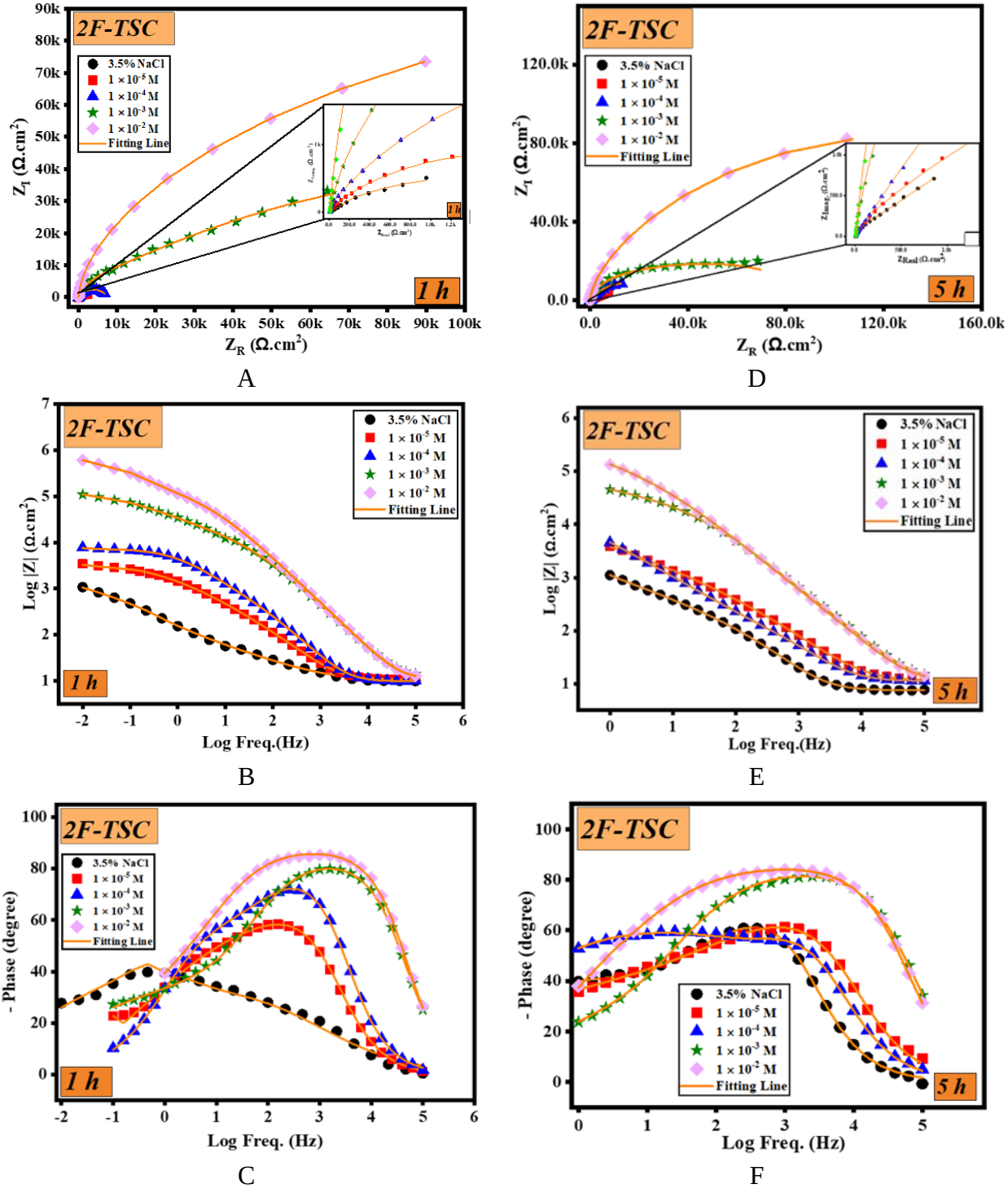

Figure 4. EIS for copper in 3.5% NaCl solution without and with the present of inhibitor 2F-TSC at immersion time 1 h (left) and 5 h (right), Nyquist plot (A), Bode plot (B-C)

utilization of the subsequent equations [29,30]:

$$IE_{PDP}\,(\%) = \frac{i^{\circ}_{corr} - i_{corr(inh)}}{i^{\circ}_{corr}} \times 100 \quad (1)$$

$$IE_{LPR}\,(\%) = \frac{R_{P\,(inh)} - R^{\circ}_{P}}{R_{P\,(inh)}} \times 100 \quad (2)$$

$$IE_{EIS}\,(\%) = \frac{R_{P\,(inh)} - R^{\circ}_{P}}{R_{P\,(inh)}} \times 100 \quad (3)$$

3.2 Electrochemical impedance spectroscopy (EIS) studies

The Nyquist and Bode plot for 2F-TSC with a submerged time of 1 hour are presented in Fig. 4(A-C, left). The present study employed a 3.5% NaCl aqueous solution, both with and without differing concentrations (10^{-5}-10^{-2} M) of 2F-TSC inhibitor. The impedance response of the Cu electrode exhibited a depressed semicircle at high frequencies, which was succeeded by a straight line at 45o at lower frequencies, as depicted in Figure 4 (A). The Warburg impedance, denoted by the symbol W, is a reliable indicator of corrosion that is predominantly controlled by diffusion. The phenomenon under consideration pertains to the transfer of electrolytic ions from the ionic bulk to the metallic substrate at the interface of Cu/electrolyte. The ions in question may include Cl^- species that are corrosive or those associated with chemical oxygen demand. The examined low-frequency range is expeditiously suppressed by the inhibitor, leading to an increase in the width of the capacitive loop in comparison to the blank solution. As depicted in Figure 4 (A), the Nyquist plot indicates that the incorporation of 2F-TSC leads to a rise in polarization resistance, thereby exhibiting a suppressive impact. The observed trend indicates that the concentration-dependent increase in the investigated inhibitors resulted in a greater polarization resistance compared to the blank solution.

Figure 4 (B-C) depicts the Bode plots for uninhibited copper and copper inhibited with varying doses of inhibitor in a 3.5% sodium chloride solution after being immersed for a duration of 1 hour. The Bode plots depicted in Figure 4 (B-C) indicate that the introduction of the inhibitor 2F-TSC resulted in a noticeable increase in the modulus of the slope impedance, |Z|, as well as the phase angle, in comparison to the uninhibited Cu. Specifically, this effect was observed in the middle-frequency regions. The findings indicate that the inhibitor's barrier of protection effectively impedes the migration of the corrosive species.

The Nyquist and Bode plots for 2F-TSC with a submerged duration of 5 hours are presented in Fig. 4(A-C, right). The 2F-TSC exhibits a fascinating result. The findings indicate that the duration of immersion has a significant impact on both the size of the impedance spectrum and the inhibition efficiency of the inhibitor. The extension of the capacitive loop was achieved through an increase in the immersion period. This resulted in the electrostatic adsorption of more succinct anions onto the positively charged copper surface, leading to more area of surface coverage and effective protection from risky ions [20,31,32].

The equivalent circuit model for copper in the presence of 2F-TSC, under both inhibited and uninhibited conditions, in a 3.5% NaCl solution is illustrated in Fig.5. The solution contains a singular model, as the impedance curves exhibited identical forms in both the presence and absence of the inhibitor. The CPE refers to a constant phase element, while the Warburg impedance is denoted by W. The variable "Rs" denotes the resistance of the solution, while "Rp" denotes the resistance of polarization. Table 2 illustrates that the Rp augmented as the inhibitor concentration increased in comparison to the blank (absence of inhibitor). This suggests a reduction in the quantity of available active sites on the Cu surface due to the adsorption of inhibitor molecules. Based on the polarization resistance Rp, which is inversely related to the corrosion rate, the inhibitor efficiency, or IE%, was calculated. The decreasing effective capacitance values (CPE) with increasing inhibitor concentration (Table 2) are due to a drop in the local dielectric constant and/or an increase in the thickness of the deposited inhibitor film. This film slows the reactions of Cu dissolution by blocking the passage of copper ions from Cu/solution contact to solution corrosion. It is noteworthy that the existence of an inhibitor results in an elevation of the n value. The observed behavior indicates a decrease in surface heterogeneity as a result of the adsorption of the inhibitor.

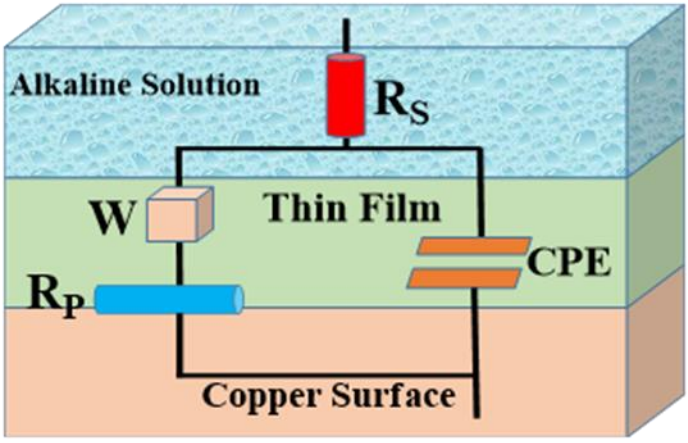

Figure 5. Equivalent circuit for copper in 3.5% NaCl solution with inhibited and uninhibited by 2F-TSC

Table 2 illustrates that the Rp values of Cu subjected to inhibition reached 209697 Ω.cm^2 after a submerged period of 5 hours in the presence of 2F-TSC, in comparison with the value of 2225 Ω.cm^2 for unprotected copper. At a concentration of 10^{-2} M 2F-TSC and an immersion time of 5 hours, the presence of an inhibitor resulted in a maximum inhibitory efficiency of 98.9%. In significantly other terms, there exists a connection between the results and the measurements of polarization.

3.3 Surface Characterization

The SEM images for copper are depicted in Figure 6. Figure 6A pertains to the sample used for polishing. The presence of a pristine copper substrate, devoid of any corrosion, alongside a smooth surface and a limited number

of horizontal and parallel scratches resulting from the polishing process, can be discerned. Figure 6 (B) demonstrates that the copper's unprotected surface (when exposed to a 3.5% NaCl solution) is highly susceptible to corrosion and weakened due to the aggressive corrosive nature of the sodium chloride solution. The topography of the copper surface exhibits undulating elevations with multiple depressions and cracks. Figure (6) denoted by the letter "C" relates to the restrained behavior of copper when exposed to 2F-TSC at a concentration of 10^{-2} M. The inclusion of an inhibitor leads to notable preservation of the substrate's copper surface and manifests a polished appearance. The observed results may be ascribed to the adsorption of inhibitor molecules onto the surface of copper, thereby hindering the dissolution of the copper surface. The composition of the Cu surface was analyzed using EDX scan measurement (as shown in Fig. 6 (A-C)) in various conditions, including before and after submerged in 3.5% NaCl, in the blank state, and in the presence of 2F-TSC. The EDX spectra presented in Figure 6(A) indicate the presence of a free corrosion substrate, as evidenced by the high peak for Cu and low peak for oxygen resulting from atmospheric exposure. Additionally, the EDX spectra obtained from the sample exposed to 3.5% NaCl (as depicted in Figure 6 (B)) reveal the existence of both Cu and a significant Cl peak on the surface. The deposition of particles on the substrate surface is attributed to the presence of corrosion products. The electrolytic inhibition of a sample using 2F-TSC has been observed to exhibit the existence of inhibitor-derived constituents, namely C, N, F, and S, as evidenced by its spectra. The data indicates a notable decrease in the peaks corresponding to chlorine and oxygen. The elevated Cu peak observed on the surface can be attributed to the presence of inhibitor molecules that have been adsorbed onto the Cu surface, thereby impeding the rate of copper dissolution [20,33].

Fig.7 (A-C) shows AFM images (2D and 3D) for the copper system. Fig.7 (A) refers to a polishing sample for copper surface, and Fig.7 (B-C) refers to uninhibited copper and the presence of 2F-TSC at concentration 10^{-2} M and immersion time 72 h, respectively. The assessment of surface roughness variability was conducted by means of two parameters, namely the average roughness (Ra) and the root mean square roughness (Rq). The aforementioned values are depicted in Figure 7 (A-C) of the present study. Figure 7 (A) demonstrates that the surface that is not immersed exhibits a notably smooth texture, devoid of corrosion and possessing minimal roughness. Figure 7 (B) depicts the surface of copper that has been exposed to an aggressive solution, exhibiting rough structures and deep, large pits that have been formed due to the aggressive attack by a 3.5% NaCl solution. Furthermore, a considerable quantity of mountains is illustrated in the 3D images of the surface, which is correlated with the surface's exposure to detrimental ions such as chlorine. Figure 7 (C) depicts the specimen that has been subjected to a solution containing an inhibitor, resulting in a notable decrease in the formation of cracks and pits. The 3D images exhibit a reduced visibility of mountains. The atomic force microscopy (AFM) images have provided information on the values of Ra and Rq. The inhibited sample exhibits a lower Ra value, indicating that the presence of inhibitor molecules on the copper surface results in a smoother surface and lower current density due to the formation of a thin film [14].

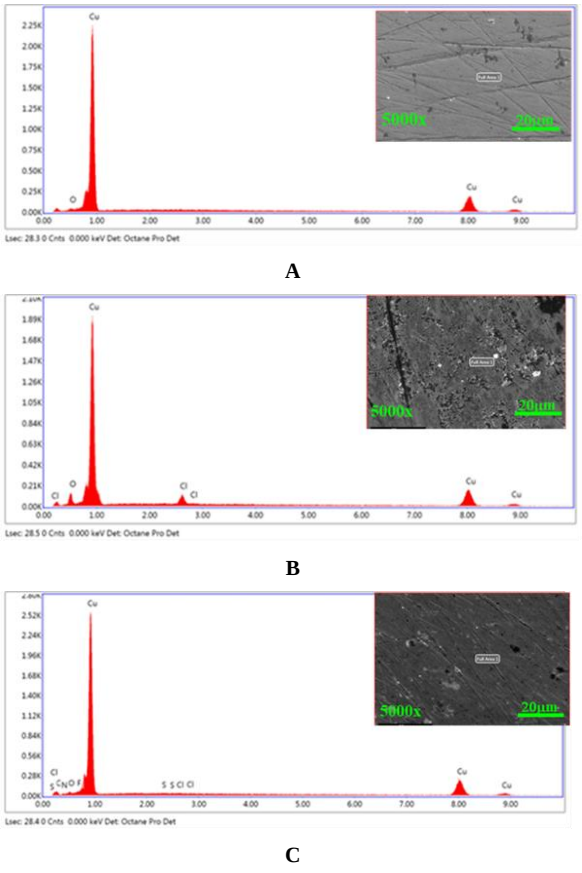

Figure 6. SEM and EDX images for copper as a polishing only (A), immersion in 3.5% NaCl (B), and immersion in 3.5% NaCl solution with the presence of 2F-TSC.

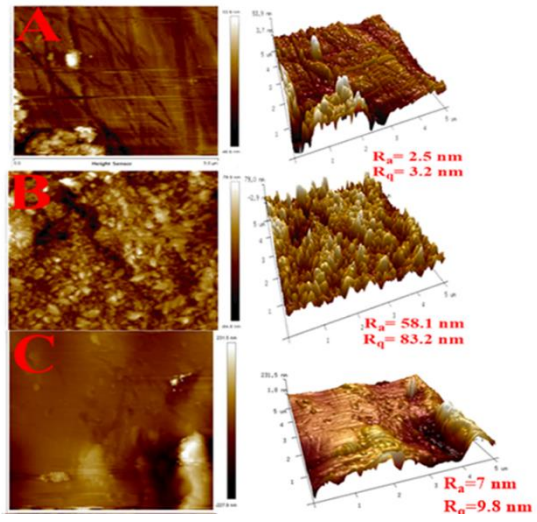

Figure 7. AFM images for copper as a polishing only (A), immersion in 3.5% NaCl (B), and immersion in 3.5% NaCl solution with the presence of 2F-TSC.

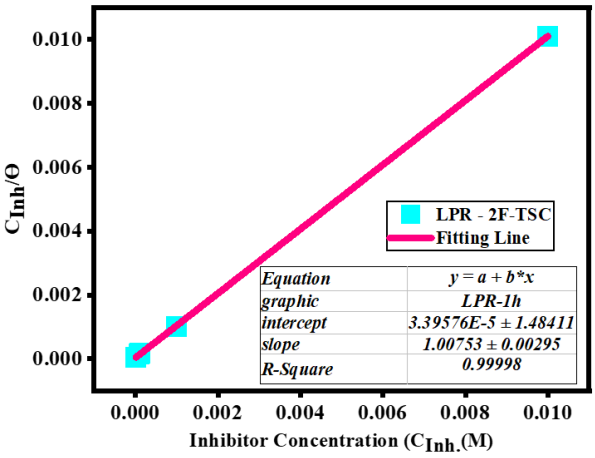

Figure 8. Langmuir adsorption isotherm of 2F-TSC on the copper surface

3.4 Adsorption isotherm

Adsorption of the investigated inhibitor on the metal surface is the most important step forward in the consumption restriction procedure. Adsorption isotherms like Langmuir's, Frumkin's, and Freundlich's are widely employed to depict the inhibitor adsorption part. The following equation depicting the Langmuir adsorption isotherm was found to be the most realistic in our study.

$$\frac{C_{inh}}{\theta} = \frac{1}{K_{ads}} + C_{inh} \quad (4)$$

Where C_{inh} is the concentration of inhibitor, θ is the level of surface inclusion by inhibitor and K is the equilibrium constant of adsorptive.

The adsorption of 2F-TSC is confirmed to follow the Langmuir isotherm by the estimate of the relationship coefficient (R^2), which is directly supported by the plotted plot of Cinh/ θ against inhibitor fixation (Cinh) (Fig. 8). R^2 values of this estimate also show that the atoms of the compound arranged themselves into a monomolecular layer on the terminal surface [34]. And here's an equation for calculating the adsorption Gibbs free energy (ΔG_{ads}):

$$\Delta G_{ads} = -RT \times \ln(55.5 \times K_{ads}) \quad (5)$$

Complete electrostatic connection (physisorption) is indicated by ΔG_{ads} values about -20 kJ mol^{-1}, whereas ΔG_{ads} values of - 40 kJ mol^{-1} or greater indicate chemical connection [35,36]. Therefore, the current study includes calculations of which - 35.4 kJ. mol^{-1} for 2F-TSC suggested the ΔG_{ads} interaction of the inhibitor with the copper surface through mixed (chemisorption and physisorption) [14].

3.5 Monte Carlo simulation studies

The equilibrium configuration of inhibitor 2F-TSC adsorbed on Cu (111) is depicted in Fig.9, featuring both side and top views. The graphical representation in Figure 9 illustrates that the inhibitor structures exhibit favorable interaction with a planar configuration on the Cu (111) surface. The adsorption process between the metal surface and inhibitor was found to occur spontaneously, as evidenced by the negative value of the adsorption energy [1]. The adsorption sites that exhibit activity are primarily localized on the nitrogen and sulfur atoms, as well as the aromatic ring. This suggests that the coexistence of an inhibitor in conjunction with aqueous conditions enhances and reinforces the adsorption mechanism. The adsorption energy value for 2F-TSC is -76.09 Kcal/mol. Consequently, the inhibitor shall undergo adsorption onto the metal surface, thereby generating substantial hydrophobic barriers that shall impede corrosion [14,20,37]. The equation presented below is used to determine the adsorption energy (Eads) of a corrosion inhibitor on metal surfaces.

$$E_{ads} = E_{total} - \left(E_{surf+water} + E_{inh+water}\right) + E_{water} \quad (6)$$

$$E_{binding} = -E_{ads} \quad (7)$$

The term E_{total} pertains to the overall energy of the system, encompassing the metal crystal, the adsorbed inhibitor molecule, and the solution. $E_{surf.+water}$ and $E_{inh+water}$ denote the potential energies of the system in the absence of the inhibitor and the metal crystal. The depiction of the potential energy of water is represented by Ewater.

This discovery provides clear evidence for the effectiveness of inhibitor 2F-TSC in inhibiting copper corrosion in a solution containing 3.5% NaCl. This implies that the results obtained from theoretical analysis are congruent with the results observed through experimentation.

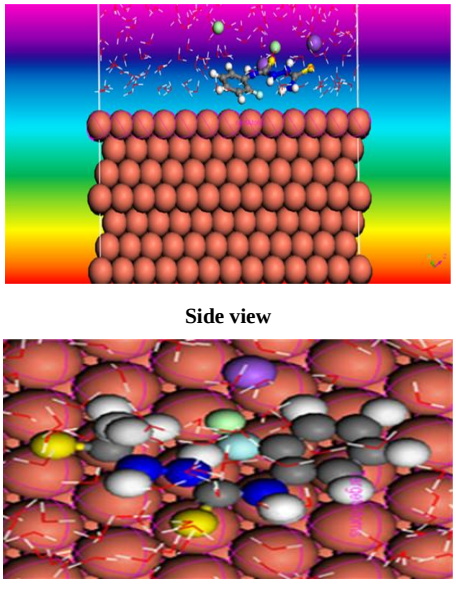

Side view

Top view

Figure 9. Side and top views of the equilibrium configuration for 2F-TSC adsorbed on Cu (111) as aqueous

4. Conclusion

Following is a statement that could be derived from the data:

- The compound 2F-TSC appeared to be an excellent corrosion inhibitor for copper in a 3.5% NaCl solution even in long-term immersion (5 h), and maximum efficiency reached 99.2% at 5 h with 10^{-2} M 2F-TSC.
- The Tafel curve illustrated that the 2F-TSC can be classified as a mix-type inhibitor
- For EIS graphs with and without 2F-TSC, there is a single equivalent circuit. The polarization resistance increases when the inhibitor is present in a 3.5% NaCl, which increases the double-layer capacitance.
- The adsorption of 2F-TSC molecules onto a copper surface is best described by the Langmuir adsorption model.
- SEM, EDX, and AFM results confirmed the presence of the inhibitor 2F-TSC on the copper surface.
- The adsorption of the inhibitor molecules on the Cu (111) surface was further verified by a Monte Carlo simulation study.

Authors' contribution

All authors contributed equally to the preparation of this article.

Declaration of competing interest

The authors declare no conflicts of interest.

Acknowledgments

The authors express their gratitude towards the Scientific Research Coordination Unit of Kastamonu University. This work has received financial support through Project number KÜ-BAP03/2020-5.

REFERENCES

[1] K. Rahmani, R. Jadidian, S. Haghtalab, Evaluation of inhibitors and biocides on the corrosion, scaling, and biofouling control of carbon steel and copper–nickel alloys in a power plant cooling water system, Desalination. 393 (2016) 174–185. https://doi.org/10.1016/j.desal.2015.07.026.

[2] M.M. Singh, R.B. Rastogi, B.N. Upadhyay, Inhibition of Copper Corrosion in Aqueous Sodium Chloride Solution by Various Forms of the Piperidine Moiety, CORROSION. 50 (1994) 620–625. https://doi.org/10.5006/1.3293535.

[3] J. Wu, X. Zheng, W. Li, L. Yin, S. Zhang, Copper corrosion inhibition by the combined effect of inhibitor and passive film in alkaline solution, Research on Chemical Intermediates. 41 (2015) 8557–8570. https://doi.org/10.1007/s11164-014-1910-4.

[4] T.D. Division, Jerzy Birn, Igor Skalski, Robert J. K. Wood, Anton Klassert, Corrosion behavior and protection of copper and aluminum alloys in seawater, First publ, WOODHEAD PUBLISHING LIMITED Cambridge England, 2003. https://doi.org/10.16309/j.cnki.issn.1007-1776.2003.03.004.

[5] P.P. Samal, C.P. Singh, S. Krishnamurthy, Expounding lemonal terpenoids as corrosion inhibitors for copper using DFT based calculations, Applied Surface Science. 614 (2023) 156066. https://doi.org/10.1016/j.apsusc.2022.156066.

[6] M. Rbaa, M. Ouakki, M. Galai, A. Berisha, B. Lakhrissi, C. Jama, I. Warad, A. Zarrouk, Simple preparation and characterization of novel 8-Hydroxyquinoline derivatives as effective acid corrosion inhibitor for mild steel: Experimental and theoretical studies, Colloids and Surfaces A: Physicochemical and Engineering Aspects. 602 (2020) 125094. https://doi.org/10.1016/j.colsurfa.2020.125094.

[7] E.A. Şahin, R. Solmaz, İ.H. Gecibesler, G. Kardaş, Adsorption ability, stability and corrosion inhibition mechanism of phoenix dactylifera extract on mild steel, Materials Research Express. 7 (2020) 016585. https://doi.org/10.1088/2053-1591/ab6ad3.

[8] Y. Xu, Q. Zhou, L. Liu, Q. Zhang, S. Song, Y. Huang, Exploring the corrosion performances of carbon steel in flowing natural seawater and synthetic sea waters, Corrosion Engineering, Science and Technology. 55 (2020) 579–588. https://doi.org/10.1080/1478422X.2020.1765476.

[9] L.O. Olasunkanmi, E.E. Ebenso, Experimental and computational studies on propanone derivatives of quinoxalin-6-yl-4,5-dihydropyrazole as inhibitors of mild steel corrosion in hydrochloric acid, Journal of Colloid and Interface Science. 561 (2020) 104–116. https://doi.org/10.1016/j.jcis.2019.11.097.

[10] L. Guo, I.B. Obot, X. Zheng, X. Shen, Y. Qiang, S. Kaya, C. Kaya, Theoretical insight into an empirical rule about organic corrosion inhibitors containing nitrogen, oxygen, and sulfur atoms, Applied Surface Science. 406 (2017) 301–306. https://doi.org/10.1016/j.apsusc.2017.02.134.

[11] C. Machado Fernandes, L. V. Faro, V.G.S.S. Pina, M.C.B.V. de Souza, F.C.S. Boechat, M.C. de Souza, M. Briganti, F. Totti, E.A. Ponzio, Study of three new halogenated oxoquinolinecarbohydrazide N-phosphonate derivatives as corrosion inhibitor for mild steel in acid environment, Surfaces, and Interfaces. 21 (2020) 100773. https://doi.org/10.1016/j.surfin.2020.100773.

[12] A. Chaouiki, M. Chafiq, H. Lgaz, M.R. Al-Hadeethi, I.H. Ali, S. Masroor, I.-M. Chung, Green Corrosion Inhibition of Mild Steel by Hydrazone Derivatives in 1.0 M HCl, Coatings. 10 (2020) 640. https://doi.org/10.3390/coatings10070640.

[13] B. Tan, B. Xiang, S. Zhang, Y. Qiang, L. Xu, S. Chen, J. He, Papaya leaves extract as a novel eco-friendly corrosion inhibitor for Cu in H2SO4 medium, Journal of Colloid and Interface Science. 582 (2021) 918–931. https://doi.org/10.1016/j.jcis.2020.08.093.

[14] M.G.K. AlFalah, F. Kandemirli, Corrosion Inhibition Potential of Dithiohydrazodicarbonamide Derivatives for Mild Steel in Acid Media: Synthesis, Experimental, DFT, and Monte Carlo Studies, Arabian Journal for Science and Engineering. 47 (2022) 6395–6424. https://doi.org/10.1007/s13369-021-06368-y.

[15] M. Ghazi, K. Alfalah, M. Abdulrazzaq, M.S. Lu, F. Kandemirli, 4-Naphthyl-3-Thiosemicarbazide as Corrosion Inhibitor for Copper in Sea Water (3.5% Sodium Chloride), Eurasian Journal of Science Engineering and Technology. 1 (2020) 27–34.

[16] M. Yadav, Retracted: Inhibition Effect of Substituted Thiadiazoles on Corrosion Activity of N80 Steel in HCl Solution, Journal of Metallurgy. 2019 (2019) 1–1. https://doi.org/10.1155/2019/1678431.

[17] M.. Singh, R.. Rastogi, B.. Upadhyay, M. Yadav, Thiosemicarbazide, phenyl isothiocyanate and their condensation product as corrosion inhibitors of copper in aqueous chloride solutions, Materials Chemistry and Physics. 80 (2003) 283–293. https://doi.org/10.1016/S0254-0584(02)00513-8.

[18] G. Latha, S. Rajeswari, Evaluation of non-ionic surfactants as corrosion inhibitors in seawater, Anti-Corrosion Methods and Materials. 43 (1996) 19–22. https://doi.org/10.1108/eb007402.

[19] E. Otero, J.M. Bastidas, Cleaning of two hundred year-old copper works of art using citric acid with and without benzotriazole and 2-amino-5-mercapto-1,3,4-thiadiazole, Materials and Corrosion/Werkstoffe Und Korrosion. 47 (1996) 133–138. https://doi.org/10.1002/maco.19960470303.

[20] M.G.K. AlFalah, L. Guo, M. Saracoglu, F. Kandemirli, Corrosion inhibition performance of 2-ethyl phenyl-2, 5-dithiohydrazodicarbonamide on Fe (110)/Cu (111) in acidic/alkaline solutions: Synthesis, experimental, theoretical, and molecular dynamic studies, Journal of the Indian Chemical Society. 99 (2022) 100656. https://doi.org/10.1016/j.jics.2022.100656.

[21] Ž.Z. Tasić, M.B. Petrović Mihajlović, M.B. Radovanović, A.T. Simonović, M.M. Antonijević, Cephradine as corrosion inhibitor for copper in 0.9% NaCl solution, Journal of Molecular Structure. 1159 (2018) 46–54. https://doi.org/10.1016/j.molstruc.2018.01.031.

[22] M.A. Amin, S.S. Abd El-Rehim, E.E.F. El-Sherbini, R.S. Bayoumi, The inhibition of low carbon steel corrosion in hydrochloric acid solutions by succinic acid, Electrochimica Acta. 52 (2007) 3588–3600. https://doi.org/10.1016/j.electacta.2006.10.019.

[23] M.G.K. AlFalah, E. Kamberli, A.H. Abbar, F. Kandemirli, M. Saracoglu, Corrosion performance of electrospinning nanofiber ZnO-NiO-CuO/polycaprolactone coated on mild steel in acid solution, Surfaces and Interfaces. 21 (2020) 100760. https://doi.org/10.1016/j.surfin.2020.100760.

[24] C. Verma, I.B. Obot, I. Bahadur, E.-S.M. Sherif, E.E. Ebenso, Choline based ionic liquids as sustainable corrosion inhibitors on mild steel surface in acidic medium: Gravimetric, electrochemical, surface morphology, DFT and Monte Carlo simulation studies, Applied Surface Science. 457 (2018) 134–149. https://doi.org/10.1016/j.apsusc.2018.06.035.

[25] H.M. Abd El-Lateef, I.M.A. Mohamed, J.-H. Zhu, M.M. Khalaf, An efficient synthesis of electrospun TiO2-nanofibers/Schiff base phenylalanine composite and its inhibition behavior for C-steel corrosion in acidic chloride environments, Journal of the Taiwan Institute of Chemical Engineers. 112 (2020) 306–321. https://doi.org/10.1016/j.jtice.2020.06.002.

[26] S. Bashir, A. Thakur, H. Lgaz, I.-M. Chung, A. Kumar, Corrosion inhibition efficiency of bronopol on aluminium in 0.5 M HCl solution: Insights from experimental and quantum chemical studies, Surfaces and Interfaces. 20 (2020) 100542. https://doi.org/10.1016/j.surfin.2020.100542.

[27] R.B. Rastogi, M.M. Singh, K. Singh, M. Yadav, Organotin Dithiohydrazodicarbonamides as Corrosion Inhibitors for Mild Steel-Dimethyl Sulphoxide Containing HCl, Portugaliae Electrochimica Acta. 23 (2005) 315–332. https://doi.org/10.4152/pea.200502315.

[28] S. Prasad, A. Bhattacharya, V.K. Verma, S. Jayanti, D.C. Rupainwar, Synthetic and Biocidal Studies on The Complexes of 1-Aryl-2,5-dithiohydrazodicarbonamide with Co(II), Cu(II), and Zn(II), Synthesis and Reactivity in Inorganic and Metal-Organic Chemistry. 22 (1992) 489–507. https://doi.org/10.1080/15533179208020225.

[29] N. Tiwari, R.K. Mitra, M. Yadav, Corrosion protection of petroleum oil well/tubing steel using thiadiazolines as efficient corrosion inhibitor: Experimental and theoretical investigation, Surfaces and Interfaces. 22 (2021) 100770. https://doi.org/10.1016/j.surfin.2020.100770.

[30] M.G. Kadhim, D.M.T. Ali, A Critical Review on Corrosion and its Prevention in the Oilfield Equipment, Journal of Petroleum Research and Studies. 7 (2021) 162–189. https://doi.org/10.52716/jprs.v7i2.195.

[31] M.M. Ibrahim, G.A.M. Mersal, A.M. Fallatah, M. Saracoglu, F. Kandemirli, S. Alharthi, S. Szunerits, R. Boukherroub, J. Ryl, M.A. Amin, Electrochemical, theoretical and surface physicochemical studies of the alkaline copper corrosion inhibition by newly synthesized molecular complexes of benzenediamine and tetraamine with π acceptor, Journal of Molecular Liquids. 320 (2020) 114386. https://doi.org/10.1016/j.molliq.2020.114386.

[32] M.E. Khalifa, I.H. El Azab, A.A. Gobouri, G.A.M. Mersal, S. Alharthi, M. Saracoglu, F. Kandemirli, J. Ryl, M.A. Amin, Adsorption behavior and corrosion inhibitive characteristics of newly synthesized cyano-benzylidene xanthenes on copper/sodium hydroxide interface: Electrochemical, X-ray photoelectron spectroscopy and theoretical studies, Journal of Colloid and Interface Science. 580 (2020) 108–125. https://doi.org/10.1016/j.jcis.2020.06.110.

[33] K. Cherrak, M.E. Belghiti, A. Berrissoul, M. El Massaoudi, M. El Faydy, M. Taleb, S. Radi, A. Zarrouk, A. Dafali, Pyrazole carbohydrazide as corrosion inhibitor for mild steel in HCl medium: Experimental and theoretical investigations, Surfaces and Interfaces. 20 (2020) 100578. https://doi.org/10.1016/j.surfin.2020.100578.

[34] K.S.M. Ferigita, M.G.K. AlFalah, M. Saracoglu, Z. Kokbudak, S. Kaya, M.O.A. Alaghani, F. Kandemirli, Corrosion behaviour of new oxo-pyrimidine derivatives on mild steel in acidic media: Experimental, surface characterization, theoretical, and Monte Carlo studies, Applied Surface Science Advances. 7 (2022) 100200. https://doi.org/10.1016/j.apsadv.2021.100200.

[35] D.A. Jones, Principles and prevention of corrosion, Prentice-Hall International, NJ, USA, (1996) Prentice-Hall International, NJ, USA.

[36] I.S.E. Meeting, European Federation of Corrosion Publications Electrochemical Approach to Selected Corrosion and Corrosion Control Studies, 1999.

[37] M. Zhang, L. Guo, M. Zhu, K. Wang, R. Zhang, Z. He, Y. Lin, S. Leng, V. Chikaodili Anadebe, X. Zheng, Akebia trifoliate koiaz peels extract as environmentally benign corrosion inhibitor for mild steel in HCl solutions: Integrated experimental and theoretical investigations, Journal of Industrial and Engineering Chemistry. 101 (2021) 227–236. https://doi.org/10.1016/j.jiec.2021.06.009.